Solid-State Electronics, 1975, Vol. 18, pp. 399–406. Pergamon Press. Printed in Great Britain

SILICON DIOXIDE MASKING OF PHOSPHORUS DIFFUSION IN SILICON

R. N. GHOSHTAGORE
Westinghouse Research Laboratories, Pittsburgh, Pennsylvania 15235, U.S.A.

(*Received* 29 *June* 1974)

Abstract—Doped oxide diffusion condition was used to diffuse P-32 radioisotope into 1100°C thermal SiO_2. Two phosphorus containing diffusing species were identified. Their diffusion characteristics were used with the literature data on the kinetics of phosphosilicate glass formation to construct a multiple-zone model of P_2O_5 diffusion into thermal SiO_2. This physical model was quantitatively verified by several types of masking experiments. In addition, the effects of dry–wet and dry–wet–dry oxidations (at 1100 and 1200°C) on the masking capability of the thermal oxides were examined.

1. INTRODUCTION

The use of an accurate thickness of masking silicon dioxide layer, with relative impermeability to most donor and acceptor impurity oxides, is the foundation of the silicon planar technology. Ever since Frosch and Derick[1] demonstrated the feasibility of SiO_2 masking of diffusion in silicon, the phenomenon has been quantitatively treated for phosphorus[2–4] and boron[4, 5], and widely used in silicon device processing. The theoretical treatments of Sah *et al.*[2], Thurston *et al.*[4] and Horiuchi and Yamaguchi[5] were based primarily on the boundary conditions of segregation of the impurity at the oxide–silicon interface and of the continuity of impurity distribution through this interface. The treatment of Allen *et al.*[3], was different in only the assumption of unit segregation coefficient. Notwithstanding these treatments and numerous other masking data in the literature, the art of masking has no physical and mathematical basis. In more recent years, several workers[6–8] have even tried to handle the masking problem by directly determining phosphorus diffusivities in amorphous SiO_2. However, the most valuable beginning in this direction is the kinetic study of phosphosilicate glass formation on silicon by Eldridge and Balk[9].

Mathematically, a similar physical situation is the diffusion from doped oxides[10, 11]. In the process of physical modeling of doped oxide diffusions, Ghoshtagore[12] found that physically realistic boundary conditions could be obtained by introducing a surface barrier rate constant of the impurity and the consideration of profile discontinuity at the interface. A critical experimental verification of such a model revealed widely different diffusion characteristics of phosphorus oxide in SiO_2 than previously predicted[2]. Furthermore, the radiophosphorus profiles in SiO_2 (doped or undoped) obtained during this work provided considerable insight into the physical processes important in developing a masking theory. In this paper an attempt will be made to develop an integrated profile of phosphorus diffusion phenomena in SiO_2, leading ultimately to technologically useful masking relationships.

2. DIFFUSION OF PHOSPHORUS IN SILICON DIOXIDE

2.1 *Experimental technique*

Using a radiophosphorus technique reported earlier[12], direct determination of phosphorus oxide diffusivity in silicon dioxide was possible for the first time. P-32 doped oxides (up to 1 μm thickness) were chemically vapor deposited at 910 ± 10°C on both 1100°C dry and wet thermal oxides grown on (111), 20–30 Ω cm (p-boron), float-zone, chem-mechanically polished, low dislocation density (<500/cm^2) silicon. Most of the thermal oxides used were about 2000 Å. Wafers were diffused at 1100, 1150, 1200, and 1250°C (~800 cm^3/min ultra-high purity argon flow) in a resistance heated furnace on a flat quartz carrier. A uniform oxide thickness area was scribed out of each sample and the oxide serially sectioned chemically at 30–40 Å/min. Each section was quantitatively counted for P-32 activity (to a reliable error of 1 per cent or less) in an automatic anti-coincidence 2π β-proportional counter until the activity of the section was near to the background. The counting data were then corrected for background, β-decay, counter efficiency and specific activity to calculate total phosphorus concentration as a function of diffusion depth.

*Wet oxides were grown by bubbling oxygen through 90°C water.

2.2 *Results*

A typical concentration profile of phosphorus oxide in 1100°C wet thermal oxide is shown in Fig. 1. It should be noted that in all cases the out-diffusion profiles were characterized by a different diffusion coefficient (at any phosphorus concentration above solid solubility [9]) than the in-diffusion profiles. Furthermore, at a fixed temperature the latter was directly proportional to the doped oxide phosphorus concentration. The out-diffusion profiles were only functions of the temperature and time of annealing.

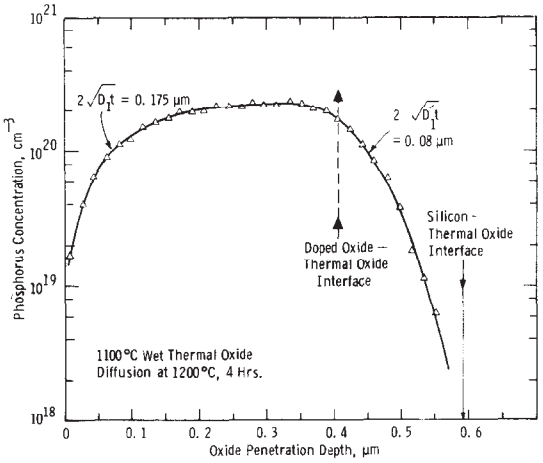

Fig. 1. Typical P-32 profile in thermal silicon dioxide.

Assuming that the evaporation rate of phosphorus to the ambient was not rate controlling, phosphorus oxide diffusivities (D_1) were calculated from the out-diffusion profiles using the relationship

$$C(x, t) = C_{ox} \operatorname{erf} \frac{x}{2\sqrt{(D_1 t)}}, \tag{1}$$

where C_{ox} is the starting doped oxide concentration. Similar concentration dependent diffusivities (D_1') were calculated from the in-diffusion profiles from the relationship

$$C(x, t) = \frac{C_{ox}}{2}\left[\operatorname{erfc} \frac{x}{2\sqrt{(D_1' t)}}\right], \tag{2}$$

assuming $x = 0$ where the phosphorus concentration drops to $C_{ox}/2$. D_1 and $D_1'(C_{ox})$ are plotted in Fig. 2 as a function of inverse absolute diffusion temperature. All the D_1' data were normalized to 1 mol % P_2O_5 doping values. The basis for such normalization is shown in Fig. 3 at 1200°C, where the apparent concentration-dependent diffusivities (D_1') determined from in-diffusion profiles

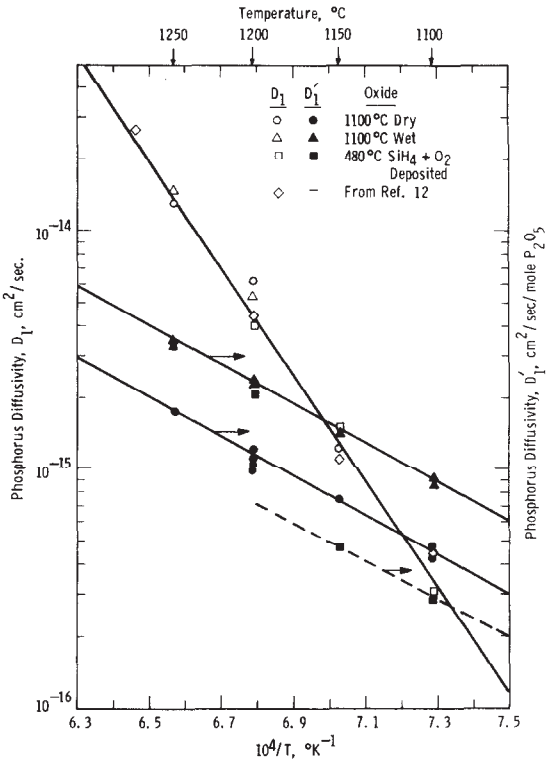

Fig. 2. Diffusivities of radiophosphorus in amorphous SiO_2 at different temperatures.

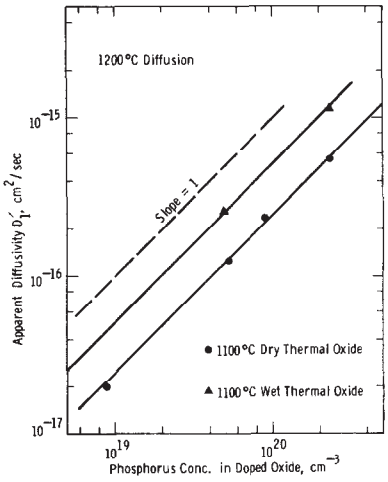

Fig. 3. Surface concentration dependence of phosphorus slow diffusivity in SiO_2 at 1200°C.

[using equation (2)] are plotted against the phosphorus concentrations in the doped oxide used. For both types of oxides used, D_1' was directly proportional to the starting phosphorus concentration. As is evident from Fig. 2, all the D_1' data for wet oxides can be represented by an

Arrhenius plot about a factor of two higher than those for dry oxides. They can be represented by the least-squares equation

$$D_1' = 4{\cdot}0(\pm 0{\cdot}1) \times 10^{-10} \exp\left[\frac{-1{\cdot}62 \pm 0{\cdot}03\ \text{eV}}{kT}\right] \text{cm}^2/\text{sec per mole} \quad (3)$$

for the 1100°C dry oxides and

$$D_1' = 8{\cdot}8(\pm 0{\cdot}2) \times 10^{-10} \exp\left[\frac{-1{\cdot}63 \pm 0{\cdot}03\ \text{eV}}{kT}\right] \text{cm}^2/\text{sec per mole} \quad (4)$$

for the 1100°C wet oxides. Similar equation for D_1 is

$$D_1 = [7{\cdot}23 \pm 6{\cdot}00] \exp\left[\frac{-4{\cdot}44 \pm 0{\cdot}23\ \text{eV}}{kT}\right] \text{cm}^2/\text{sec}. \quad (5)$$

2.3 *Mechanism of phosphorus diffusion in thermal SiO_2*

Proper identification of the structural nature of the diffusing species responsible for equation (3)–(5) is rather arbitrary at present. The faster species (above 1150°C) has about three times the diffusion activation energy of the slower species and a pre-exponential term more indicative of solid state diffusion [equation (5)]. Over and above, this is the rate determining unit in both out-diffusion from doped oxide films (under liquidus composition) and in doping Si by the doped oxide process[12]. Below ~0·5 mole % concentration of P_2O_5 in SiO_2, this unit also possesses concentration independent diffusivity in SiO_2. Commensurate with all these characteristics, this species is suggested to be P_2O_5 (solid).

On the other hand, the slower species not only possess diffusion parameters [equations (3) and (4)] characteristic of a liquid in a solid, its diffusivity is very matrix structure sensitive (Fig. 2). At any temperature, it exists between only two fixed concentration points of liquidus composition and the solid solubility of P_2O_5 in SiO_2 (see later). Its diffusivity is a first order monotonic function of its surface concentration (Fig. 3). Consequently, it can best be designated as a fixed composition 'liquid' ($xP_2O_5 \cdot ySiO_2$). Traces of moisture greatly affect its mobility (by the formation of a hydrated species, perhaps). Conceptually, this liquid species should also be responsible for out-diffusion from doped oxide films seen in section 2. However, volatile P_2O_5, formed by decomposition of this species at the surface, effectively controls this out-diffusion profile.

It is possible to conceive a third elemental phosphorus (or phosphorus in an oxidation state lower than +5) diffusing species in SiO_2. This is probably the species involved in all tracer data available in the literature[6–8], where the experiments were conducted under non-oxidizing conditions from elemental phosphorus. In all technological processes, the existence of this third species in sufficient concentrations to control phosphorus diffusion rate in SiO_2 is, however, highly improbable.

3. DEVELOPMENT OF MASKING RELATIONSHIPS

3.1 *Background information on the phosphosilicate system*

Any successful model of the diffused structure of phosphosilicate glass on silicon has to consider the following:

(a) recognize the wide variety of diffusivity data of phosphorus in SiO_2 available in the literature[2–4, 6–8, 11, 12];

(b) include the kinetic concept of phosphosilicate glass formation painstakingly developed by Eldridge and Balk[9], and

(c) use the tracer diffusivity data of phosphorus oxide in SiO_2 obtained in this study.

The available phosphorus diffusivity data in SiO_2 can be classified into (i) those indirectly obtained from the diffusion characteristics of phosphorus in silicon through a thermal barrier oxide[2–4] or from the doped oxide[11, 12], and (ii) those obtained from radiotracer study[6–8]. All the indirect phosphorus oxide diffusivity data in SiO_2 were obtained by assuming a model of dopant segregation at the SiO_2–Si interface. In the light of the recent discredit to such a physical situation[12], all these data could be temporarily ignored. However, since such indirect data obtained from the doped oxide diffusion study both with[11] or without[12] the segregation coefficient concept seem to be validated by the present tracer study, they need be included into the development of the present model. On the other hand, all the literature P-32 tracer diffusivity values[6–8] in SiO_2 are for the elemental species and, consequently, unrelated to the standard process (open tube or doped oxide) masking criteria.

Using the standard open tube $POCl_3$ diffusion system with dry 1100°C thermal SiO_2 layers, Eldridge and Balk[9] established the kinetics of phosphosilicate glass (PSG) formation over a wide range of temperatures (800–1200°C). The formation of PSG layers was characterized by elegant etch rate profiles. They defined the thickness of the PSG layer (l_{PSG}) as that up to the point in SiO_2 where P_2O_5 concentration is equal to its solid solubility. Their data can be expressed by the relationship

$$l_{PSG} = \{9{\cdot}032(\pm 0{\cdot}170) \times 10^6\}\{\sqrt{(C_p t)}\} \exp\left(\frac{-0{\cdot}815\ \text{eV}}{kT}\right) \text{Å}, \quad (6)$$

where T is the temperature of annealing (°K), t is the

duration of annealing (sec), and C_p is the phosphorus concentration in the gas phase (vol. %).

3.2 *Physical modeling of the phosphosilicate system*

Now, with equations (3)–(6) and some reasonable assumptions, one can proceed to construct a physical model of the diffused phosphosilicate glass system. This will be accomplished in this section.

If l_{PSG} can be considered to be the sum of a surface liquid PSG layer, l_1^m (at appropriate diffusion conditions), and a 'liquid' ($xP_2O_5 \cdot ySiO_2$) permeated solid SiO_2 layer, l_2^m, then

$$l_{PSG} = l_1^m + l_2^m. \tag{7}$$

If one further assumes that D_1' [Equation (3) or (4)] controls the formation of this second layer, l_2^m of equation (7) can be calculated (at any temperature) from the tracer in-diffusion data reported in section 2 with appropriate modification for the liquidus composition. At any temperature (above ~850°C) this region has a phosphorus profile given by the relationship

$$l_2^m = 2\sqrt{(D_1't)}\,\text{argerfc}\left(\frac{N_s}{N_L}\right), \tag{8}$$

where N_S is the solid solubility of P_2O_5 in SiO_2, N_L is the liquidus composition, and D_1' is the concentration dependent diffusivity in dry 1100°C thermal SiO_2 [given by equation (3)].

Numerical values of N_S, N_L, and D_1', to be used with equation (8) and determined by Eldridge and Balk[9], are given in Table 1. Using calculated values of l_{PSG} from equation (6) and l_2^m from equation (8), l_1^m can be obtained from equation (7).

In the absence of any available kinetic and thermodynamic data for the 1100°C *wet thermal oxide*, it is, however, necessary to assume that the same N_S and N_L values (Table 1) can be used in this case. Furthermore, if it is assumed that at any fixed temperature l_1^m is identical for both the dry and wet 1100°C thermal oxides, l_{PSG} for the wet 1100°C oxide system can be calculated from the sum of l_1^m and the calculated l_2^m for the wet oxide. In this case, l_2^m is obtained from equation (8) with concentration dependent D_1' given by equation (4).

The technologically important quantity of the minimum oxide thickness required to prevent the formation of a junction into silicon, the *masking thickness*, can now be expressed by

$$l^m = l_{PSG} + l_3^m, \tag{9}$$

where l_3^m is the layer formed by diffusion of P_2O_5 into SiO_2 (below the maximum solid solubility controlled concentration N_S of P_2O_5 in SiO_2) according to the corrected Batdorf and Smits[13] relationship

$$l_3^m = \frac{2D_1t}{l_{PSG}} \ln \frac{N_S}{N_C}, \tag{10}$$

where D_1 is the concentration independent diffusivity of P_2O_5 in SiO_2, and N_C is a critical P_2O_5 concentration in SiO_2 at the SiO_2–Si interface. D_1 is given by equation (5) and has also been determined from the doped oxide diffusion study[12]. For a given *p*-type silicon substrate, N_C is defined by that concentration of P_2O_5 in SiO_2 which produces a phosphorus concentration on the Si surface (during a very short annealing time) equal to the background concentration and can be found from ref. [12]. For an *n*-type substrate, it can be defined as that P_2O_5 concentration in SiO_2 which produces a negligible surface concentration in silicon after a very short annealing time. It can be easily shown that l_3^m is negligible compared to l_1^m and l_2^m. Consequently, equation (9) reduces to

$$l^m = l_1^m + l_2^m = l_{PSG}. \tag{11}$$

The above hypothesized physical model of the diffused phosphosilicate system is diagrammatically depicted in Fig. 4. As will be proven later by the masking experiments (section 3.3), this is the structure of the multiphase system normally obtained by open tube deposition process. This structure can also be obtained under doped oxide drive-in conditions if the doped oxide composition is over the liquidus (N_L) composition at the drive-in temperature (e.g., emitter diffusions). However, if the doped oxide

Table 1. Data on the PSG system[9]

Temp. (°C)	Solid solubility of P_2O_5 in SiO_2 (N_S) (mol % P_2O_5)	(P_2O_5 (cm^{-3})	Liquidus composition (N_L) (mol % P_2O_5)	Effective diffusivity, D_1', of $xP_2O_5 \cdot ySiO_2$ 'Liquid' at liquidus composition (cm^2/sec)
1100	$1{\cdot}09 \times 10^{-2}$	$2{\cdot}50 \times 10^{18}$	10·0	$4{\cdot}045 \times 10^{-15}$
1150	$1{\cdot}37 \times 10^{-2}$	$3{\cdot}15 \times 10^{18}$	8·3	$5{\cdot}453 \times 10^{-15}$
1200	$1{\cdot}70 \times 10^{-2}$	$3{\cdot}90 \times 10^{18}$	6·7	$6{\cdot}919 \times 10^{-15}$
1250	$2{\cdot}09 \times 10^{-2}$	$4{\cdot}80 \times 10^{18}$	5·2	$8{\cdot}192 \times 10^{-15}$

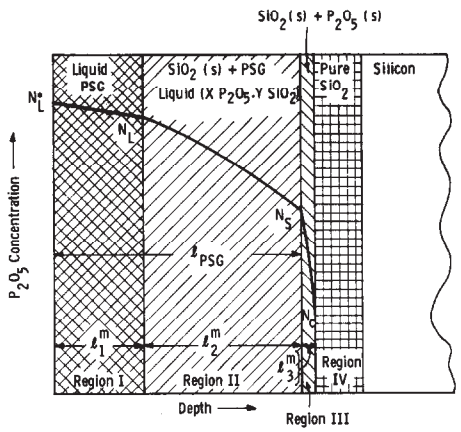

Fig. 4. Diagrammatic representation of the phosphosilicate glass structure on silicon. See test for explanation.

composition (N_0) is below N_L, no liquid is formed, and such PSG layers are devoid of region I in Fig. 4. In such a case, l_2^m is given by

$$l_2^m = 2\sqrt{(D_1't)}\,\text{argerfc}\left(\frac{N_S}{N_0}\right), \tag{12}$$

instead of equation (8), and D_1' (for either dry or wet 1100°C oxide) must also be calculated for N_0. Consequently, for such doped-oxide diffusions,

$$l^m = l_2^m. \tag{13}$$

3.3 *Masking experiments*

3.3.1 *Experimental technique.* The theory of masking of phosphorus diffusion for thermal SiO_2 developed in section 3.2 was critically evaluated for both the open tube phosphorus deposition (using phosphine source and the doped-oxide deposition (using predeposited P_2O_5 doped SiO_2 film source). Masking ability of three types of thermal SiO_2 layers (dry, wet and dry–wet–dry), grown at two different temperatures (1100° and 1200°C), were quantitatively evaluated. These masking oxides were grown on 20–30 Ω cm, boron-doped, float-zoned, (111) ± 2°, one side chem-mechanically polished, 10–12 mils thick, 1–1/2 in. dia., low dislocation density (<500 cm^{-2}) silicon. The wet oxides were grown with the first 10 min in dry oxygen and the rest in oxygen bubbled through 90°C water. In the case of dry–wet–dry oxides, the wet thermal oxides were dehydrated by annealing in dry nitrogen for 10 min before removal from the furnace. All the three types of oxides were grown in pairs of thicknesses ~100 Å apart in the range 1200–6000 Å. For each experiment, the mask failure condition was set in the middle of each pair of thicknesses. Consequently, the minimum accuracy of l^m determination was ±50 Å at any oxide thickness. All the oxide thicknesses were determined from a color chart prepared from the same type of oxide by ellipsometry. To check the validity of the experimental relationships at large thicknesses, a few oxide thicknesses were prepared (dry–wet–dry) in the 15–18 kÅ and 25–30 kÅ range. For both the open tube and doped oxide experimental conditions the mask failure criterion was set at that point in diffusion time when the silicon substrate (of a pair of thicknesses ~100 Å apart) with the lower oxide thickness showed any n-type spot anywhere on its surface (with a hot probe) while the other remained completely p-type. More than 75 per cent of the masking experiments were repeated for reproducibility checks.

All the open tube diffusion experiments were conducted in a 55 mm i.d. quartz tube in a resistance heated furnace with a thermal flat of <1°C over 18 in. Nitrogen was used as the carrier gas with a total flow of 1 l/m. The ratio of O_2 to PH_3 flow rates was always maintained at 37·5. All the oxidized wafers were preheated for 2 min (on a flat quartz carrier) before the reactant gases were admitted. The post-diffusion flush time of one minute was included in the total deposition time. Since equation (6) was originally determined [9] for gas phase phosphorus concentration dependence with $POCl_3$, all the open tube masking experiments performed in this work were with phosphine [to check the universal validity of equation (6)]. Two phosphine concentrations of 0·04 and 0·09 vol. % were used in this work at two different temperatures (1150° and 1200°C).

For the doped oxide experiments, a semi-infinite layer (1·1 ± 0·1 μm) of 5·15 mole % P_2O_5 doped SiO_2 was grown at 480°C from SiH_4, PH_3, and O_2 in N_2 carrier gas in an r.f.-heated reactor. The composition of the doped oxide was calibrated from radiotracer data reported earlier [12]. This particular composition was chosen for the express purpose of avoiding the formation of a liquid PSG surface layer even at the highest annealing temperature in this study (see Table 1). In addition, this experimental condition would be capable of validating the concept of l_2^m assumed and developed in section 3.2. Using all the types of thermal oxides under investigation, doped oxide diffusion experiments were performed at both 1100° and 1200°C.

3.3.2 *Results with 1100°C thermal oxide.* Figure 5 shows the minimum oxide thickness required (l^m) for successful masking (at 1150° and 1200°C) of phosphorus as a function of the square root of the deposition time. The continuous lines are theoretical values obtained from equations (6) and (11). Both at 1150° and 1200°C, the 1100°C dry thermal oxide is much superior to the 1100°C wet thermal oxide in masking ability. Furthermore, it is clear that those last 10 min of dry nitrogen dehydration (after oxidation) of 1100°C wet thermal oxide has raised its masking ability to

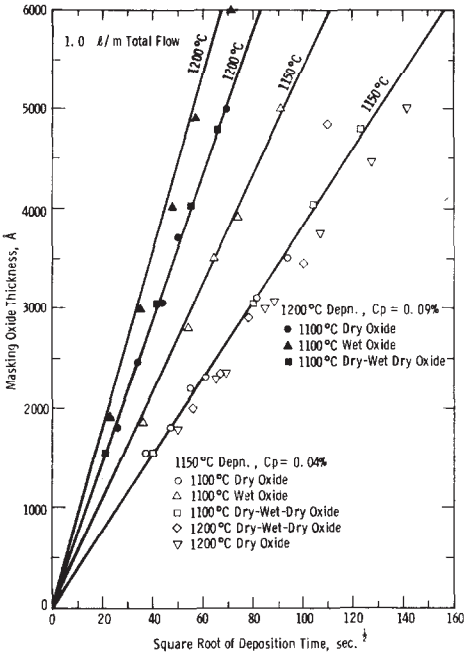

Fig. 5. Masking relationships for the open tube phosphine deposition process.

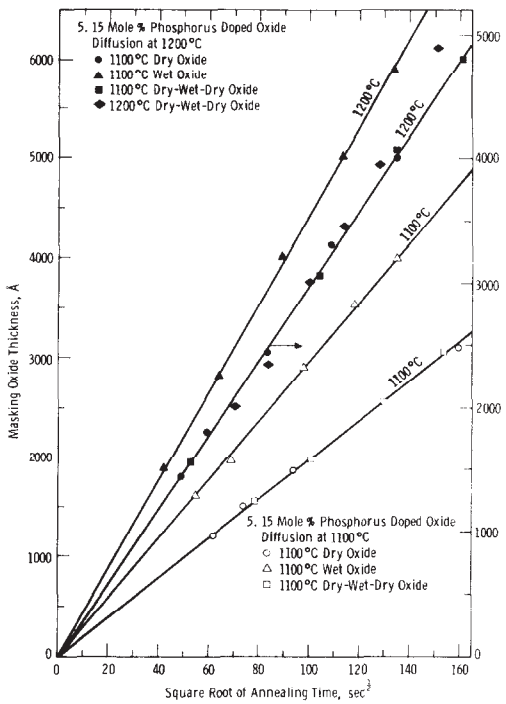

Fig. 6. Masking relationships for the doped oxide diffusion process.

that of the dry oxide. It should, however, be noted that phosphorus penetration of wet oxide and, to some extent, dry–wet–dry oxide was considerably spottier than the dry oxide. The excellent experimental validation of the present masking theory is evident from Figs. 5 and 6.

Figure 6 shows masking data for the 5·15 mole % phosphorus doped oxide diffusion process at 1100° and 1200°C. The continuous theoretical lines are from equations (12) and (13). Here again the dry oxide is superior to the wet oxide by the same extent and the dry–wet–dry oxide is identical to the dry oxide. In other words, under identical conditions, both the dry and wet oxides form the same amount of region I (Fig. 4) and they are only different in forming region II. That quantitatively translates to the difference of equations (3) and (4), i.e., the concentration dependent diffusivity D_1' of the $xP_2O_5 \cdot y\,SiO_2$ 'liquid' is enhanced by a factor of about two by the water vapor retained in wet 1100°C thermal oxides. Any structural or kinetic explanation for this effect is not evident.

3.3.3 *Results with 1200°C thermal oxide.* Masking data for the 1200°C dry and dry–wet–dry thermal oxides are included in Figs. 5 and 6. Under both open tube and doped oxide diffusion conditions, the 1200°C dry thermal oxide is seen to possess at least as good a masking ability as the 1100°C dry oxide, if not slightly better. However, the situation is quite different for the 1200°C dry–wet–dry oxide. Figure 6 shows that the masking ability of such oxides is non-linear with the square root of annealing time and becomes increasingly inferior with thickness or oxidation time. Since the last dry cycle (during oxidation) was enough to remove all water vapor from the oxide film at 1100°C, it is reasonable to assume that this was so at 1200°C. Then the obvious explanation for such behavior of the 1200°C dry–wet–dry oxide is the water vapor catalyzed partial crystallization at 1200°C, either from the free surface or from the SiO_2–Si interface.

To distinguish either of these possibilities, some masking experiments were performed with 1200°C dry and dry–wet–dry oxides at 1150°C by the open tube method (0·04 vol. % PH_3) and at 1200°C by the doped oxide process (5·15 mole % P_2O_5). These data are shown in Fig. 7. It should be pointed out that the designed difference between these two types of masking experiments were the formation of a liquid PSG layer by the former. Figure 7 shows that the masking inferiority of the 1200°C dry–wet–dry oxide (compared to that of the 1200°C dry oxide) starts at a smaller thickness for the doped oxide process than that in the open tube process (even with allowance for the difference in diffusion temperatures). If the dissolution of some SiO_2 from the free surface by the formation of liquid PSG layer is considered for the open tube process, it can be concluded that the partial crystallization of the 1200°C dry–wet–dry

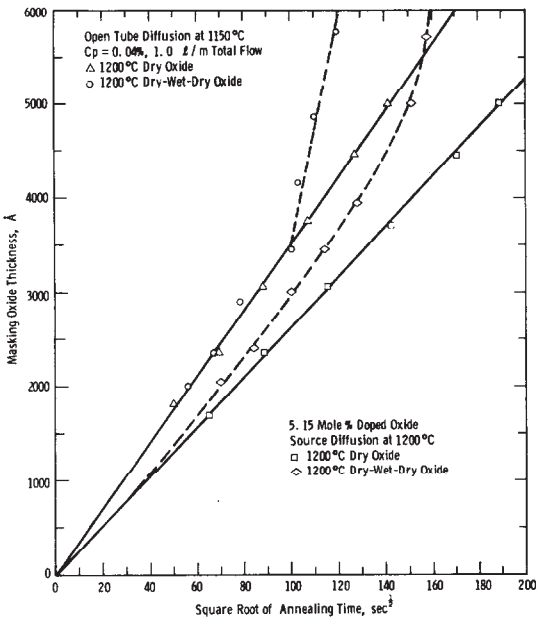

Fig. 7. Masking relationships for the 1200°C thermal oxide.

oxide (with the aid of water vapor) starts from the free surface inwards and not from the Si–SiO_2 interface outwards. In any case, the 1200°C moisture assisted oxidation is definitely harmful to the masking ability of the oxide against P_2O_5. No further effort was made in modeling these so-called partially crystallized SiO_2 films with faster crystalline and/or grain-boundary diffusion of $xP_2O_5 \cdot ySiO_2$ 'liquid.' Since no additional insight was expected by using 1200°C wet oxides, no phosphorus masking experiments were performed with them.

3.4 *Discussion of the masking model*

The correctness of the two species model of P_2O_5 diffusion in thermal SiO_2, developed in section 3.2 and illustrated in Fig. 4, has been satisfactorily validated in the above-described masking experiments. In addition, the masking property of thermal SiO_2 has been successfully explained by a physical model comprised essentially of three different phases of so-called 'phosphosilicate glass' on silicon. The first phase on the surface is a layer of SiO_2 containing P_2O_5 concentrations above the liquidus composition (described by the P_2O_5–SiO_2 phase diagram) at the diffusion temperature. Consequently, it is a high viscosity liquid layer with either a nearly constant P_2O_5 concentration profile (in the case of diffusion from doped oxides of appropriate concentrations) or a linearly decreasing (inwards) P_2O_5 concentration profile (in the case of most open tube depositions) ending at the liquidus composition. The formation rate of this layer is only dependent on the P_2O_5 concentration (external or internal) and temperature.

The second phase under this PSG liquid layer is comprised of solid SiO_2 and a fixed composition phosphosilicate ($xP_2O_5 \cdot ySiO_2$) 'liquid.' Whereas the first completely liquid PSG layer is formed only when the surface P_2O_5 concentration is above the liquidus, this second phase is almost always formed in doped oxide and open tube phosphorus diffusions. This phase is internally bounded at that point in SiO_2 where P_2O_5 concentration equals to its solid solubility. The rate of formation of this mixed phase layer is proportional to the square root of its surface concentration (always between the liquidus and solid solubility compositions). It also depends on the type of SiO_2 matrix used (thermal or deposited, moisture content, and crystallinity). Using the formation rate of this layer, it has been established that (1) wet thermal oxide is inferior to the dry thermal oxide in masking ability because of the difference in the thickness of this second layer formed, (2) wet oxide can be made equivalent to the dry oxide in masking ability by approximately a minimum of 10 min of dehydration at 1100°C in dry nitrogen, and (3) appreciable crystallization of SiO_2 takes place during wet oxidation at 1200°C near the free surface. Depending on the particular oxidizing diffusion condition employed, this second layer may constitute the major part of the PSG layer formed.

Third phase layer is a solid solution of P_2O_5 in SiO_2 and is formed right near the SiO_2–Si interface. Because of the very low solid solubility of P_2O_5 in thermal SiO_2[9] at most commonly used diffusion temperatures, and because of the silicon surface barrier rate constant limiting transfer of phosphorus into silicon[12], the role of this third solid layer in masking is negligible compared to the first two.

4. SUMMARY

Using radiotracer techniques to diffuse phosphorus from a semi-infinite 910°C deposited doped SiO_2 layer into 1100°C thermal (wet and dry) silicon dioxide, two diffusing species of phosphorus oxide in SiO_2 have been identified. The faster species (above 1150°C) has been tentatively labeled as the solid state diffusion of P_2O_5 in SiO_2 and can be described by the equation

$$D_1 = [7{\cdot}23 \pm 6{\cdot}00] \exp\left(\frac{-4{\cdot}44 \pm 0{\cdot}23\ \text{eV}}{kT}\right) \text{cm}^2/\text{sec}.$$

This species is rate-controlling in the out-diffusion of phosphorus and in the doping of silicon from doped oxide sources (below liquidus composition)[12]. It has a negligible role in mask failures. The second slower species has been tentatively identified with a fixed composition 'liquid' ($xP_2O_5 \cdot ySiO_2$) diffusing through a solid SiO_2

matrix. Its diffusivity is surface concentration dependent and can be described by the equation

$$D_1' = 4{\cdot}0(\pm 0{\cdot}1) \times 10^{-10} \exp\left(\frac{-1{\cdot}62 \pm 0{\cdot}03\ \text{eV}}{kT}\right)$$

cm^2/sec per mole P_2O_5 surface concentration in the 1100°C dry thermal oxide and by the equation

$$D_1' = 8{\cdot}8(\pm 0{\cdot}2) \times 10^{-10} \exp\left(\frac{-1{\cdot}63 \pm 0{\cdot}03\ \text{eV}}{kT}\right)$$

cm^2/sec per mole P_2O_5 surface concentration in the 1100°C wet thermal oxide.

With the help of these radiotracer data, the phosphosilicate glass formation kinetic data of Eldridge and Balk[9] has been reinterpreted to produce a three-zone multiphase model of phosphosilicate glass on thermal SiO_2. According to this model, the first zone is a liquid phosphosilicate layer with or without a constant concentration gradient to the liquidus composition. From then on to the point of solid solubility composition in SiO_2 is the second zone of solid SiO_2 permeated by a constant composition phosphosilicate 'liquid' ($xP_2O_5 \cdot ySiO_2$). The third zone is due to the solid state diffusion of P_2O_5 in SiO_2 and is unimportant in magnitude (compared to the first two zones) for masking purposes. For an open tube oxidizing phosphorus deposition from the gas phase (or semi-infinite doped oxide source diffusion above the liquidus composition), if l_1^m and l_2^m are the thicknesses of these two primary PSG zones, then the masking thickness, l^m, i.e., the minimum oxide thickness required to prevent the formation of a junction into silicon, was found to be

$$l^m = l_1^m + l_2^m = \{9{\cdot}032(\pm 0{\cdot}170) \times 10^6\} \times \{\sqrt{(C_p t)}\} \exp\left(\frac{-0{\cdot}815\ \text{eV}}{kT}\right) \text{Å} \qquad (6)$$

where C_p is the volume phosphorus concentration in the gas phase (per cent), and t is the deposition time at the temperature T.

If no liquid layer (l_1^m) is formed (as in some doped oxide processes),

$$l^m = l_2^m = 2\sqrt{(D_1' t)}\ \text{argerfc}\left(\frac{N_s}{N_0}\right) \qquad (12)$$

where D_1' is the effective diffusivity of the constant composition liquid PSG ($xP_2O_5 \cdot ySiO_2$) at the doped oxide (or surface) phosphorus concentration N_0 and N_s is the corresponding solid solubility of P_2O_5 in SiO_2.

Masking experiments performed with both the doped oxide source and the open tube $PH_3 + O_2$ source (at two compositions and three temperatures in the range 1100–1200°C) satisfactorily agreed with equations (6) and (12). It was further established that 1100°C wet oxides are inferior masks due to larger l_2^m layer formed, that they can be made equivalent to dry oxides in masking capability by a simple dry nitrogen baking at the end of the oxidation cycle, and that 1200°C dry–wet–dry oxides are inferior masks than either 1100 or 1200°C dry oxides most possibly due to partial surface crystallization.

Note added in proof. A more rigorous description of l_2^m (equations (8) and (12)) would be the application of Batdorf and Smits moving boundary condition[13] to region II in the form of equation (10). Numerically, such l_2^m would be imperceptibly smaller than the l_2^m given by equations (8) and (12) and the validation of masking data (Fig. 6 and 7) virtually unaffected.

REFERENCES

1. C. J. Frosch and L. Derick, *J. Electrochem. Soc.* **104**, 547 (1957).
2. C. T. Sah, H. Sello and D. A. Tremere, *J. Phys. Chem. Solids* **11**, 288 (1959).
3. R. B. Allen, H. Bernstein, and D. A. Kurtz, *J. appl. Phys.* **31**, 334 (1960).
4. M. O. Thurston, J. C. C. Tsai and K. D. Kang, *Final Report, Diffusion of Impurities into Silicon through an Oxide layer*, Ohio State Univ. Res. Foundation, AD-261201, Contract DA-36-039-SC-83874, Columbus, Ohio (1961).
5. S. Horiuchi and J. Yamaguchi, *Jap. J. appl. Phys.* **1**, 314 (1962).
6. Y. Watanabe and M. Yoshida, *Jap. J. appl. Phys.* **6**, 410 (1967).
7. L. Ke-Cheng, X. Shi-Yin, Z. Shong-de and H. Yun, *Acta Phys. Sinica* **20**, 496 (1965).
8. D. R. Campbell, E. I. Alessandrini, D. N. Tu and J. E. Lewis, *142nd National Electrochem. Soc. Meeting*, Miami Beach, Florida, Abstract No. 252 (1972).
9. J. M. Eldridge and P. Balk, *Trans. AIME* **242**, 539 (1968).
10. M. L. Barry and P. Olofsen, *J. Electrochem. Soc.* **116**, 854 (1969).
11. M. L. Barry, *J. Electrochem. Soc.* **117**, 1405 (1970).
12. R. N. Ghoshtagore, *Solid-St. Electron.* **17**, 1065 (1974).
13. R. L. Batdorf and F. M. Smits, *J. appl. Phys.* **30**, 259 (1959).